



HAL
open science

Study of the Ge₂₀Te_{80-x}Sex glassy structures by combining solid state NMR, vibrational spectroscopies and DFT modelling

C. Gonçalves, R. Mereau, Virginie Nazabal, Catherine Boussard-Plédel, Claire Roiland, E. Furet, M. Deschamps, B. Bureau, M. Dussauze

► To cite this version:

C. Gonçalves, R. Mereau, Virginie Nazabal, Catherine Boussard-Plédel, Claire Roiland, et al.. Study of the Ge₂₀Te_{80-x}Sex glassy structures by combining solid state NMR, vibrational spectroscopies and DFT modelling. *Journal of Solid State Chemistry*, 2021, 297, pp.122062. 10.1016/j.jssc.2021.122062 . hal-03196087

HAL Id: hal-03196087

<https://hal.science/hal-03196087v1>

Submitted on 16 Apr 2021

HAL is a multi-disciplinary open access archive for the deposit and dissemination of scientific research documents, whether they are published or not. The documents may come from teaching and research institutions in France or abroad, or from public or private research centers.

L'archive ouverte pluridisciplinaire **HAL**, est destinée au dépôt et à la diffusion de documents scientifiques de niveau recherche, publiés ou non, émanant des établissements d'enseignement et de recherche français ou étrangers, des laboratoires publics ou privés.

Study of the $\text{Ge}_{20}\text{Te}_{80-x}\text{Se}_x$ glassy structures by combining solid state NMR, vibrational spectroscopies and DFT modelling

Claudia Gonçalves^{1,2}, *Raphaël Mereau*², *Virginie Nazabal*^{1,*}, *Catherine Boussard-Pledel*¹,
*Claire Roiland*¹, *Eric Furet*³, *Michaël Deschamps*⁴, *Bruno Bureau*¹, *Marc Dussauze*^{2,*}

¹ Institut des Sciences Chimiques de Rennes, UMR 6226 CNRS, Equipe Verres & Céramiques, Université Rennes 1, Campus de Beaulieu, 35042 Rennes, France

² Institut des Sciences Moléculaires, Université de Bordeaux, CNRS UMR 5255, F-33400 Talence, France

³ Institut des Sciences Chimiques de Rennes, UMR 6226 CNRS, Ecole Nationale Supérieure de Chimie de Rennes, 35708 Rennes, France

⁴ CNRS, CEMHTI UPR3079, Orléans University, Orléans 45100, France

Credit Author Statement:

Claudia Gonçalves, Catherine Boussard-Pledel and Claire Roiland, have been involved in the materials synthesis.

Claudia Gonçalves and Marc Dussauze have achieved the Raman and IR characterizations.

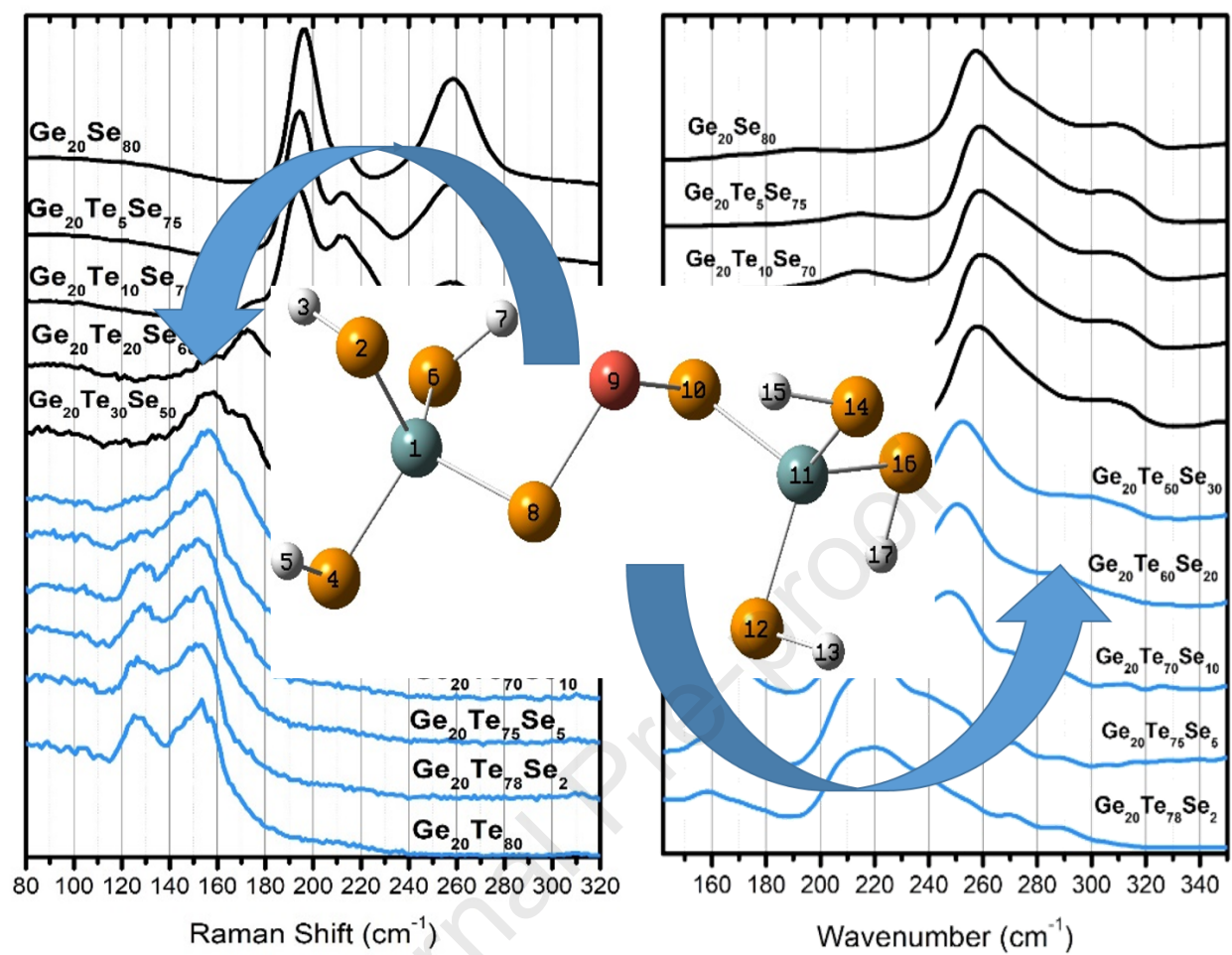
Claudia Gonçalves, Michaël Deschamps and Bruno Bureau were in charge of the NMR measurements.

Raphaël Mereau, Eric Furet and Marc Dussauze were involved in the choice of the DFT clusters.

Raphaël Mereau was responsible of the DFT calculations.

Claudia Gonçalves, Virginie Nazabal, Bruno Bureau and Marc Dussauze were in charge of the data interpretation.

Claudia Gonçalves, Virginie Nazabal, Bruno Bureau and Marc Dussauze have written the text of the manuscript.



Study of the Ge₂₀Te_{80-x}Se_x glassy structures by combining solid state NMR, vibrational spectroscopies and DFT modelling

Claudia Gonçalves^{1,2}, Raphaël Mereau², Virginie Nazabal^{1,}, Catherine Boussard-Pledel¹,
Claire Roiland¹, Eric Furet³, Michaël Deschamps⁴, Bruno Bureau¹, Marc Dussauze^{2,*}*

¹ Institut des Sciences Chimiques de Rennes, UMR 6226 CNRS, Equipe Verres & Céramiques,
Université Rennes 1, Campus de Beaulieu, 35042 Rennes, France

² Institut des Sciences Moléculaires, Université de Bordeaux, CNRS UMR 5255, F-33400
Talence, France

³ Institut des Sciences Chimiques de Rennes, UMR 6226 CNRS, Ecole Nationale Supérieure de
Chimie de Rennes, 35708 Rennes, France

⁴ CNRS, CEMHTI UPR3079, Orléans University, Orléans 45100, France

KEYWORDS. Chalcogenide glasses, Structure, ss-NMR spectroscopy, Vibrational spectroscopies, DFT modelling

ABSTRACT: The glassy ternary system Ge-Te-Se is currently receiving an increased attention due to its extended range of transmission in the infrared opening the way to various potential applications in photonics. In this study, a multi-techniques approach combining solid-state NMR, Raman and infrared spectroscopies and DFT calculations provides insight into the organization

of the $\text{GeSe}_4\text{-GeTe}_4$ glassy network and allows to clarify a whole structural description of the glassy system. A particular attention is devoted to the presence of mixed $\text{GeTe}_{8-x}\text{Se}_x$ structural units and to the type of interconnections forming the glass networks. Such experimental/theoretical approach is provided both for the selenium and the tellurium rich part of the glassy system.

1. INTRODUCTION

The first studies on the Ge-Te-Se ternary glassy system presenting an extensive vitreous domain were focused on the thermal and electrical properties.[1,2] It is only with the growing interest in information storage that these glasses have been considered for their phase change properties.[3–5] Recently, Ge-Te-Se glasses have been investigated for space and biological research.[6,7] Indeed, chalcogenide glasses are known for their extended range of transmission in the infrared (up to a wavelength of 14 μm for bulk selenide glasses with thicknesses of few mm, and even beyond wavelength of 18 μm for telluride glasses). Several studies are still going on to further extend the transmission range of these glasses. It is the reason why tellurium-rich glasses have been the subject of much work in recent years.

Despite a smaller range of transparency, selenide glasses are known to synthesize easily, with a broad vitreous domain. They have been the subject of numerous experimental and theoretical studies, particularly for GeSe_4 and GeSe_2 by NMR and Raman spectroscopies, neutrons and density-functional based molecular dynamics simulations.[8–13]. In $\text{Ge}_x\text{Se}_{100-x}$ glasses, the dominant coordination number for Ge is four and Se is two, and coordination defects would also be present for these two atoms in a small proportion. The Ge five-fold coordinated would be less

than 5%, while the Ge and Se three-fold coordinated would be even smaller but would increase for GeSe₂ glass to ~11 and 8%, respectively[12]. In the case of stoichiometric GeSe₂ glass, the [GeSe_{4/2}] tetrahedral (Td) can be linked by corners (CS) or an edge (ES). In addition, the presence of Ge-Ge (forming (GeGeSe₃) entities only) and Se-Se homopolar bonds allowed by the relatively close electro-negativities of Ge and Se atoms are expected and probably over- or under-coordinated atoms as well, as mentioned. For GeSe₄ in particular, the occurrence of a fully bonded network is suggested, in which Se-Se-Ge linkages ensure the connection between Se-Se-Se chains and Ge-Se-Ge tetrahedral arrangements[11]. The proportion of these [GeSe_{4/2}] Td CS and ES motifs, homopolar bonds and coordination defects evolve according to the composition of the Ge_xSe_{100-x} glasses forming odd- and even-sized rings.

In order to take advantage of the structural similarities between tellurium and selenium, research was then conducted along the pseudo-binary line GeSe₄-GeTe₄ (i.e. Ge₂₀Se_{80-x}Te_x) of the Ge-Te-Se ternary diagram, in order to find the best compromise between the wide GeTe₄ transparency window and the ease of synthesis and shaping of GeSe₄. Maurugeon *et al.*[6] showed that the addition of a small percentage of selenium in the vitreous matrix of Ge-Te system stabilized the material and kept the extended range of transparency characteristic of telluride glasses. It is important to mention that beyond $x = 30$ and before $x = 50$, there is a non-mixing zone, where it seems extremely delicate to form glass under conventional synthesis conditions.

A number of structural analyzes have already been done on this Ge-Te-Se ternary system. Either the work focused on a single composition of the ternary system, or on its selenium or tellurium-rich part. For instance, the study conducted by Jovari *et al.*[14] on the tellurium-rich part began by investigating the structure of Ge₂₀Se₁₀Te₇₀ glass by X-ray and neutrons diffraction and

Extended X-Ray Absorption Fine Structure (EXAFS) measurements, producing data simultaneously fitted by the Reverse Monte-Carlo (RMC) simulation technique. These results show that the glass is built up of $\text{Ge}(\text{Te}, \text{Se})_4$ tetrahedra linked by Te–Te and Te–Se bonds. The coordination number of Ge is close to 4, the Te is predominantly two-fold coordinated and a coordination number of Se higher than 2 is also compatible with their model. Moreover, some Se atoms in the model are shared by two $\text{Ge}(\text{Te}, \text{Se})_4$ tetrahedra without forming Te–Se bonds. To go further using the same approach, Ratkai *et al.*[15] have tried to understand the presence of the non-mixing zone for $\text{Ge}_{20}\text{Se}_{80-x}\text{Te}_x$ ($x = 75, 70, 65, 60$) glasses. They suggested that for lower Se concentration, the structure can be described as essentially built up of GeTe_4 tetrahedra connected to each other by Te–Te dimers. Se preferentially binds to Ge for all compositions investigated. From 20% of Se, Se–Se bonds start to be present without Se–Te bonding and the Te–Te coordination starts to increase. For this concentration, nanoscale phase separation is envisaged due the fact that Se and Te avoid each other in the presence of Ge. Lately, studies have been carried out to explore the crystal growth process that limits the fiber-drawing procedure for the tellurium-rich glasses (up to 10 at.% of Se) [16–18]. They confirmed that selenium atoms will bind preferentially to Ge atoms and proposed, based on Raman spectroscopy investigation, an increase with Se addition in the amount of edge-shared tetrahedra and the short Te chains interconnecting the tetrahedral networks, excluding the presence of GeSe_4 tetrahedra and Se_n chains.

On the selenium-rich part of the system, Moharram *et al.*[19] studied four compositions $\text{Ge}_{20}\text{Se}_{80-x}\text{Te}_x$ ($x = 0, 10, 20$ and 30) by XRD technique and Raman spectroscopy considering the chemical order network model approach.[19] They concluded with the presence of mixed chalcogenide chains interconnecting the germanium tetrahedral. $\text{GeTe}_{4/2}$ entities are proposed to

be excluded from their Raman spectroscopy analysis. Recently, NMR studies on Ge-Te-Se glasses with have been carried out to understand the structure of the vitreous network. Bouëssel du Bourg *et al.*[20] studied the impact of tellurium on the structure of selenium-rich part of the GeSe₄-GeTe₄ pseudo-binary line (i.e. Ge₂₀Se_{80-x}Te_x, x = 0, 10, 30 and 60). This study, comparing experimental and theoretical results, concluded that Ge atoms are mainly 4-fold coordinated with a single maximum centered at 109° for the angular distribution functions and that a single tellurium at the maximum can be found in its coordination sphere with a very low occurrence. This analysis of the molecular dynamics structures has shown that the Te atoms avoid binding to Ge atoms. The tellurium would rather disperse in the selenium chains, which causes a subsidence of the number of Se-Se-Se environment.

In the present study, we have focused our attention on the structure of the entire pseudo-binary GeSe₄-GeTe₄ glassy system. We will present the results of ⁷³Ge solid-state NMR characterizations and IR / RAMAN vibrational spectroscopies measurements combined to DFT calculations.

2. EXPERIMENTAL SECTION

Glass Preparation

Ge₂₀Te_{80-x}Se_x glasses (with x varying from 0 to 80) were prepared in silica tubes, sealed under vacuum from high purity Te (6N, JX Nippon Mining), Se (5N, Umicore) and Ge (5N, Umicore) in the exact appropriate stoichiometry. The initial chemicals were not further purified before being introduced into the silica set-up. The tubes were placed into a rocking furnace at 800°C, to homogenize the melt. Then the batch is annealed for 2h (at T_g-10°C) in order to remove residual

stress and finally cooling down slowly to the room temperature. The amorphous character of samples was verified by X-ray diffraction (XRD) and Differential Scanning Calorimetry (DSC).

Solid-State NMR measurements

A series of ^{73}Ge NMR measurements were acquired on a 20T NMR spectrometer (850 MHz for ^1H and 29.66 MHz for ^{73}Ge – spin $I = 9/2$, natural abundance = 7.76%–), and in static conditions inside a 5 mm diameter solenoid probe. The chemical shift was referenced to $\text{Ge}(\text{OCH}_3)_4$. The pulse sequence was a QCPMG sequence (Quadrupolar Carr-Purcell-Meiboom-Gill echo sequence) with a 90° RF pulse of 2 μs (with a 600 W output power from the RF amplifier) that is selective on the central transition (no contribution is observed from the satellite transition). The echo delay between consecutive 180° pulses was set to 700 μs to allow for the recording of the entire full echo signal. Each Free Induction Decay (FID) signal was stored in a 2D buffer and FT was performed in a 2D mode as described elsewhere[21]. The recovery delay was set to 0.5 s for full relaxation, and Double Frequency Sweep (DFS) was used to enhance the intensity of the central transition signal[22]. The line widths remain considerable (although 1000 ppm correspond to 30 kHz) and when needed, the Variable Offset Cumulative Spectrum (VOCS) technique is used to acquire the spectra due to their broadening.[23]

Raman measurement

Raman spectroscopy measurements were carried out using the 785 nm laser on a Labram HR spectrometer, equipped with one filter which allow a global reflection of the laser for measurement in microscopy (NoiseBlock ASE Suppressor filter, Ondax®) and two SureBlock Notch filters (Ondax®) to have a sufficient optical density over a short spectral range). The acquisition of Raman spectra was, therefore, made with caution due to the photosensitive nature of the glasses. To avoid any modification of the network, it was necessary to use very low laser

powers (from 24 μW to 170 μW) as well as to apply low counting times per point. The spectra presented in this article are the average of 10 measurements, for 3 acquisitions of several minutes by points. The overall acquisition was approximately 60 minutes per spectrum.

Infrared measurement

Infrared spectra were conducted by specular reflection method on a Bruker Vertex 70V vacuum spectrometer, equipped with a mercury source, producing radiation in the far infrared. The spectral range of study is from 30 to 1000 cm^{-1} . The signal was recorded with the help of an external reflection tool with an almost normal angle of incidence (11°). The results were subjected to the Kramers-Kronig analysis, to obtain the complex refractive index (n , k). The spectra will be presented in the form of absorption coefficient $\alpha=4\pi k/\lambda$. [24]

DFT calculation

Studies of optimizations and harmonic vibrational frequency calculations were carried out on small sized clusters using Density Functional Theory (DFT) calculations, using the functional B3LYP. Prior to any geometry optimizations, the dangling bonds originating from singly bonded chalcogen atoms were neutralized by adding hydrogen-like atoms with masses equal to germanium to provide better agreement between calculated and experimental vibrational frequencies. After geometry optimizations of the clusters, harmonic vibrational frequencies were calculated from the equilibrated geometries of the different clusters, in order to obtain the Raman and Infrared spectra. Qualitative vibrational assignments were made by visualizing the atom displacement vectors for each mode likely responsible for experimental IR and Raman bands. All calculated vibrational modes including the dangling bonds of the clusters were not taken in account. In addition, a Potential Energy Distribution (PED) analysis was performed to also

quantify the contribution of internal coordinates to a specific vibrational mode. The germanium, gallium and selenium atoms have been treated by the "all-electron" 6-311 ++ G (3df, 2p) basis set except for tellurium which was treated with the help of pseudo-potential, LANL2DZ. All the calculations presented in this article were performed using the Gaussian 09 software.

2. RESULTS: EXPERIMENT

2.1. NMR results

The ^{73}Ge nucleus is not that present in literature because it combines several difficulties: low natural abundance (7.76%), low gamma ($-0.936 \times 10^7 \text{ rad} \cdot \text{T}^{-1} \cdot \text{s}^{-1}$) and a high quadrupolar constant ($-19.6 \times 10^{-30} \text{ m}^2$). This nucleus is a real challenge to probe. Three compositions were probed. The ^{73}Ge QCPMG NMR spectra are gathered in the Figure 1.

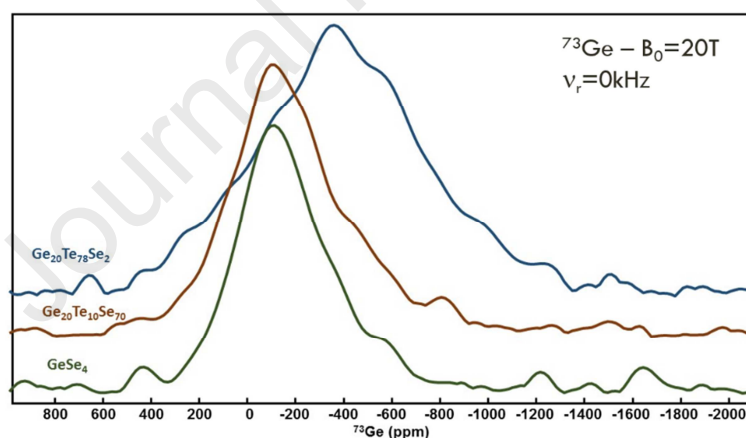


Figure 1. ^{73}Ge QCPMG NMR spectra of $\text{Ge}_{20}\text{Te}_{80-x}\text{Se}_x$ glasses (with $x = 2, 70, 80$).

The first observation is that the introduction of 10 mol.% of tellurium which replaces selenium in $\text{Ge}_{20}\text{Se}_{80}$ does not modify the shape and the position of the ^{73}Ge spectra. For the tellurium-rich glass characterized, the barycenter is shifted by 400 ppm, indicating the difference in

displacement between a tetra-coordinated tellurium germanium in comparison with a selenium-coordinated germanium.

At this stage, the observed enlargement for $\text{Ge}_{20}\text{Te}_{80}$ versus $\text{Ge}_{20}\text{Se}_{80}$ remains difficult to interpret. This broadening is certainly related to the quadrupole distribution parameter of ^{73}Ge which is stronger in the presence of tellurium than in the presence of selenium. Two simple hypotheses are possible.

First, the presence of Ge-Ge homopolar bonds within the tetrahedron was identified by Sen *et al.*[25] If this structural arrangement is to be found in the glass, it means germanium may be bound to either another germanium or Te/Se. Such a variety of coordination environments is certainly likely to widen the ^{73}Ge spectrum.

A second hypothesis is based on the greater variability in the symmetry of the GeTe_4 tetrahedra compared to the GeSe_4 tetrahedra due to the higher polarizability of tellurium: such a theory will be preferred at this stage as it does not require extensive homopolar Ge-Ge bonding in the sample.

2.2. Results on Vibrational Spectroscopy/DFT calculations

The Raman and Infrared (IR) spectra of $\text{Ge}_{20}\text{Te}_{80-x}\text{Se}_x$ (with x from 0 to 80) glasses are presented in Figure 2.

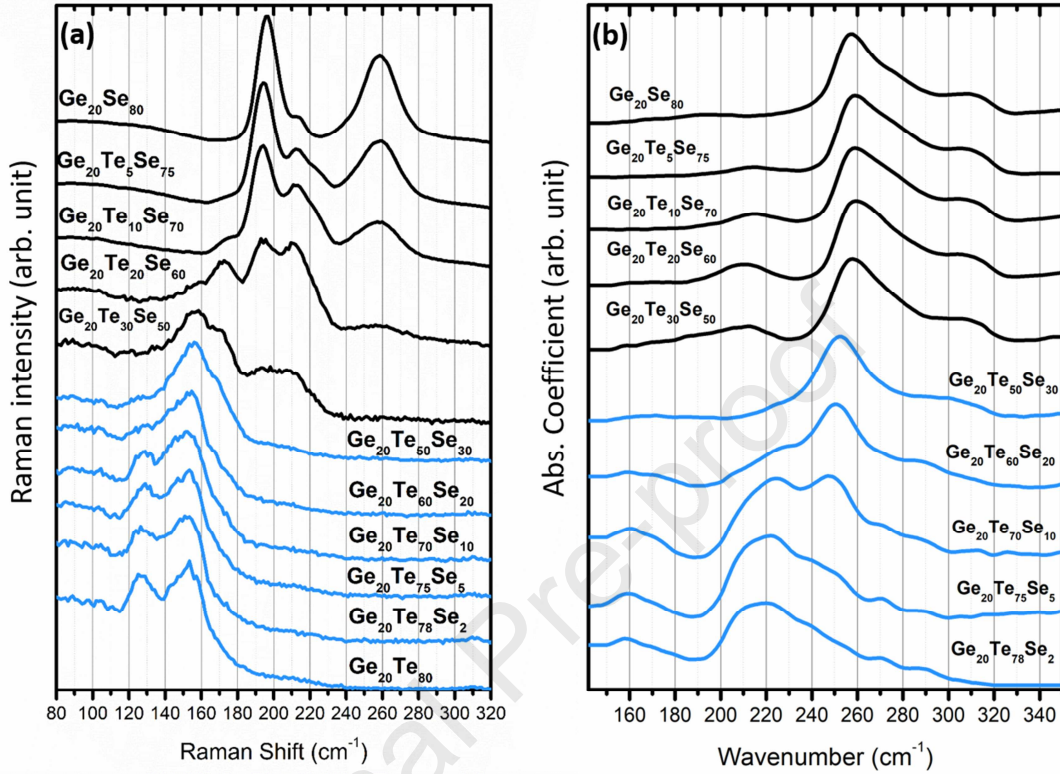


Figure 2. (a) Unpolarized Raman spectra and (b) Infrared spectra of Ge₂₀Te_{80-x}Se_x glasses.

Regarding the compositional evolution of the Raman spectra (Figure 2a.), starting from Ge₂₀Te₈₀, two contributions are observed at 126 and 155 cm⁻¹. The peak at 126 cm⁻¹ decreases by the selenium addition, until the Ge₂₀Te₅₀Se₃₀ composition where it ends up disappearing. The peak at 155 cm⁻¹ seems to widen by the addition of selenium towards higher frequencies making it asymmetrical. When the evolution of the spectra is examined starting from Ge₂₀Se₈₀, three contributions are observed at 190, 210 and 260 cm⁻¹. The addition of tellurium in the vitreous matrix reduces the peak at 260 cm⁻¹. The shoulder observed at 210 cm⁻¹ intensifies by the addition of tellurium. A new vibration mode is recorded at 170 cm⁻¹, starting from Ge₂₀Te₅Se₇₅,

and intensifies by the tellurium addition in the matrix. One can also note the shoulder at 155 cm^{-1} beginning to appear for the composition $\text{Ge}_{20}\text{Te}_{30}\text{Se}_{50}$.

For the selenium-rich part of the infrared spectra (Figure 2.b), there is no notable change. Two principal peaks are identifiable at 260 and 310 cm^{-1} and do not change to a significant degree with the tellurium addition in the matrix. It is necessary to wait for the $\text{Ge}_{20}\text{Te}_{60}\text{Se}_{20}$ composition to start observing significant differences in the spectrum. However, from 5% of tellurium in the selenium matrix, a new low intensity band can be observed for low frequency range at 210 cm^{-1} . On the other hand, in the tellurium-rich part, significant modifications are observable. A wide band at 220 cm^{-1} is recorded, extended on a broad frequency range where several contributions can be suspected. At 250 cm^{-1} , a new peak is recorded, starting from the $\text{Ge}_{20}\text{Te}_{70}\text{Se}_{10}$ composition, and increase until the non-mixing zone at $\text{Ge}_{20}\text{Te}_{50}\text{Se}_{30}$.

Few results are present in the literature to help us explaining the two tendencies observed. Either the work focused on a single composition of the Ge-Te-Se ternary system, or on a selenium or tellurium rich part of the system along the pseudo-binary line $\text{GeSe}_4\text{-GeTe}_4$. [15–19,21,26] However, different assignments of vibration bands have been reported showing the difficulties of interpretations. To interpret these results, the methodology used combine experimental acquisitions (Raman and IR) and DFT calculations on selected clusters to help in the assignment of the vibrational modes observed. Initially, we will make sure that DFT calculations can describe correctly binary glasses $\text{Ge}_{20}\text{Se}_{80}$ and $\text{Ge}_{20}\text{Te}_{80}$. The spectral refinement on this study will focus both (i) on the local stretching modes of tetrahedral units and (ii) on the vibration due to their interconnection.

2.2.1. Binary glasses $\text{Ge}_{20}\text{Se}_{80}$ and $\text{Ge}_{20}\text{Te}_{80}$

- $\text{Ge}_{20}\text{Se}_{80}$

$\text{Ge}_{20}\text{Se}_{80}$ glass presents three principal peaks in Raman spectra: 195, 210 and 260 cm^{-1} . According to the literature, these modes are assigned respectively to the symmetrical stretching of the GeSe_4 tetrahedra, the symmetrical stretching of the GeSe_4 edge-sharing tetrahedra, and finally, the stretching of the Se-Se homopolar bond into chains of variable length.[8,21] In the infrared spectrum, two broad peaks are apparent at 255 and 320 cm^{-1} , mainly due to the observation of asymmetrical stretching modes of the GeSe_4 tetrahedra.

Figure 3 shows the representative clusters of the GeSe_4 glass structure used for DFT calculations, i.e. (a) $[\text{GeSe}_4]$ tetrahedra and its Se-Se bonds, the Se-Se interconnections of varying length between two $[\text{GeSe}_4]$ tetrahedral : (b) $[\text{Ge-Se-Se-Ge}]$, (c) $[\text{Ge-Se-Se-Se-Ge}]$, and (d) $[\text{Ge-Se-Se-Se-Se-Ge}]$ and finally two $[\text{GeSe}_4]$ tetrahedra linked by the same edge forming (e) $[\text{Ge}_2\text{Se}_6]$ entities. The active modes in Raman and IR calculated by DFT from these clusters, are presented in the Table 1. The “Potential Energy Distribution” (PED) give the relative weight of each vibration describing the stretching mode of the clusters (Table 1).

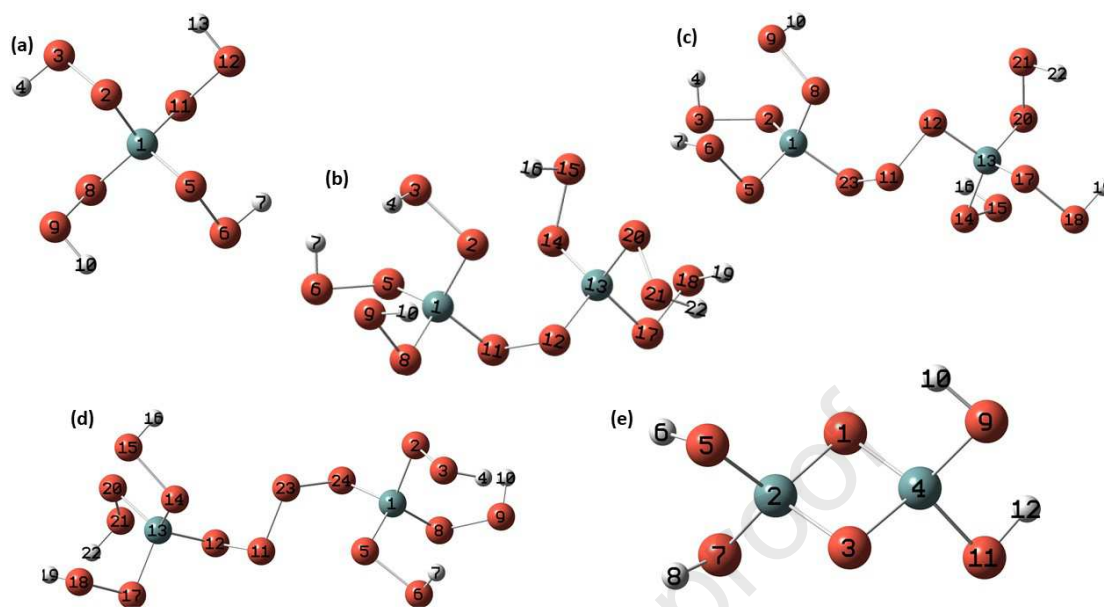


Figure 3. DFT-optimized geometries of (a) $[\text{GeSe}_4]$, (b) $[\text{Ge-Se-Se-Ge}]$, (c) $[\text{Ge-Se-Se-Se-Ge}]$, (d) $[\text{Ge-Se-Se-Se-Se-Ge}]$ and (e) $[\text{Ge}_2\text{Se}_6]$ clusters.

Table 1. Selected Raman and infrared-active vibrational modes calculated by DFT for $[\text{GeSe}_4]$ cluster, long-chain clusters and edge-sharing tetrahedral clusters shown in Fig. 3 and the relative weight of each individual vibration extracted from a Potential Energy Distribution analysis.

Calculated Frequency (cm^{-1})	Vibrational Mode	PED (%)	Cluster
187	$\nu_s \text{GeSe}_4$	$\nu(1,2)$: 16,1%, $\nu(1,5)$: 16,1%, $\nu(1,8)$: 16,1%, $\nu(1,11)$: 16,1%	Cluster a
215	$\nu_s \text{GeSe}_4$ (Edge-Sharing)	$\nu(2,1)$: 4,9%, $\nu(2,3)$: 6,9%, $\nu(2,7)$: 6,7%, $\nu(2,5)$: 6,6%, $\nu(4,1)$: 8,6%, $\nu(4,3)$: 5,0%, $\nu(4,9)$: 5,8%, $\nu(4,11)$: 5,0%	Cluster e
245	$\nu(\text{Se})\text{-Se-Se-(Se)}$	$\nu(11,23)$: 21,0%, $\nu(12,11)$: 11,1%, $\nu(23, 24)$: 11,8%	Cluster d
252	$\nu_{as} \text{Se-Se-Se}$	$\nu(12,11)$: 10,9%, $\nu(11,23)$: 12,4%	Cluster c

258	$\nu_{as} \text{GeSe}_4$	$\nu(1,2): 16,4\%, \nu(1,5): 16,4$	Cluster a
263	$\nu(\text{Se})\text{-Se-Se-(Ge)}$	$\nu(12,11): 12,3\%, \nu(23, 24) : 13,2\%, \nu(11, 23): 12,2\%$,	Cluster d
265		$\nu(11,12): 15,1\%, \nu(11,23): 4,9\%$	Cluster c
270	$\nu\text{Se-Se}$	$\nu(11,12): 17,4\%$	Cluster b
285	$\nu_{as} \text{GeSe}_4$ (Edge-Sharing)	$\nu(1,2) : 9,0\%, \nu(4,11) : 8,6\%$ $\nu(4,3) : 6,8\%, \nu(2,3) : 5,5\%$	Cluster e
311		$\nu(4,3) : 10,1\%, \nu(2,3) : 10,5\%$	
299	$\nu_{as} \text{GeSe}_4$	$\nu(1,2): 12,2\%, \nu(1,5): 12,2\%$, $\nu(1,8): 12,2\%, \nu(1,11): 12,2\%$	Cluster a

According to DFT calculation, the active mode of stretching tetrahedra calculated at 187 cm^{-1} and 215 cm^{-1} from cluster (a) and (e), respectively, can be attributed to those observed in Raman spectra of the $\text{Ge}_{20}\text{Se}_{80}$ glass. Thus, the main band at 195 cm^{-1} is associated to symmetric stretching modes of $[\text{GeSe}_4]$ tetrahedra while the shoulder observed on the Raman spectrum at 210 cm^{-1} can be associated with the symmetrical vibration modes of tetrahedra linked by an edge (Figure 4).

Concerning infrared results, the apparent maxima at 260 and 310 cm^{-1} in the infrared spectra can be related to asymmetrical stretching vibration modes of the $[\text{GeSe}_4]$ tetrahedra of cluster (a) and cluster (e) (Figure 4). More to the point, the calculated asymmetrical stretching modes at 258 cm^{-1} and 299 cm^{-1} of classical $[\text{GeSe}_4]$ tetrahedral (cluster a) mainly contribute to the main band at 260 cm^{-1} and broad band at 310 cm^{-1} (Figure 4). The calculated modes at 285 and 311 cm^{-1} represent the two asymmetrical stretching modes, both present on infrared spectra (Figure 4), of the cluster (e), i.e. corresponding to the $[\text{GeSe}_4]$ tetrahedra connected by an edge.

Considering the clusters (b, c and d) with chains of two, three and four selenium inter-connecting the $[\text{GeSe}_4]$ tetrahedra, the selected vibrational mode of Se-Se bonds will range from 245 to 270 cm^{-1} , depending on the length of chain. PED analysis shows that for short chains containing only two selenium the calculated frequency is 270 cm^{-1} while for a longer chain, represented by cluster (d), the spectroscopic signature of $\nu_s(\text{Se})\text{-Se-Se-(Se)}$ was extracted at 245 cm^{-1} . This is even more noticeable with the mode $\nu_s(\text{Se})\text{-Se-Se-(Ge)}$, where their frequencies are higher (263, 265 cm^{-1}) than the $\nu_s(\text{Se})\text{-Se-Se-(Se)}$ mode (245 cm^{-1}). To sum-up, the longer the $(\text{Se-Se})_n$ chain, the lower the frequency is, whereas a Se-Se bond linked to one or two germaniums will see its calculated frequency of vibration gradually increase.

The $\text{Ge}_{20}\text{Se}_{80}$ Raman spectrum has a broad band centered at 260 cm^{-1} usually associated with the vibrational modes of Se-Se small chains (Figure 4). The width of this band ranging from 240 to 280 cm^{-1} can be perfectly explained by bearing in mind the spread of DFT calculated frequency of the Se-Se vibration modes strongly impacted by chain length and atomic mass effect.

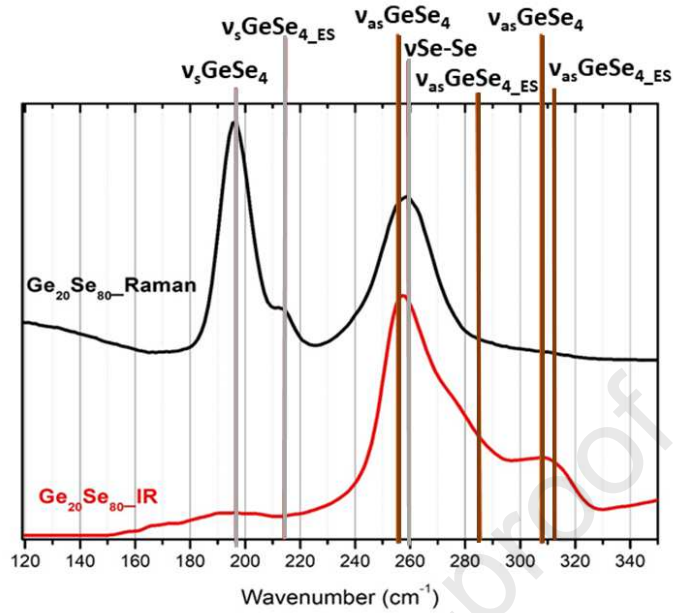


Figure 4. Assignments of vibration modes for IR and Raman spectra of $\text{Ge}_{20}\text{Se}_{80}$ glass.

- $\text{Ge}_{20}\text{Te}_{80}$

The Raman spectrum of $\text{Ge}_{20}\text{Te}_{80}$ glass is shown in Figure 6 where two main modes have been observed at 126 and 155 cm^{-1} in accordance with the literature[26,27]. Due to its high reflectivity behavior, the IR spectrum of the $\text{Ge}_{20}\text{Te}_{80}$ glass could not be recorded. The composition of $\text{Ge}_{20}\text{Te}_{78}\text{Se}_2$ was then chosen to assign the IR modes as the composition is very close to $\text{Ge}_{20}\text{Te}_{80}$. From this IR spectrum, a main wide band centered at 220 cm^{-1} was identified.

Using the same methodology than for DFT calculations of the $\text{Ge}_{20}\text{Se}_{80}$ glass, a stoichiometric cluster $[\text{GeTe}_4]$ was calculated (Figure 5a.) as well as GeTe_4 tetrahedra interconnected by chains of two, three, and four tellurium (Figure 5b. c. d. respectively). The increase of the tellurium chain will show the effect on the frequency calculation for the homopolar Te-Te bond vibration.

The results of the DFT calculation presented in Table 2 reveal a main active Raman mode at 131 cm^{-1} and two main active IR modes at 216 and 232 cm^{-1} related to the symmetrical and

antisymmetrical stretching of the GeTe_4 tetrahedra (cluster (a)), respectively. Thus, the ν_s GeTe_4 tetrahedra mode can be associated to the Raman band at 125 cm^{-1} (Figure 6). while the other two ν_{as} GeTe_4 tetrahedra modes can be observed in the infrared wide band peaking at 220 cm^{-1} and presenting a shoulder around 240 cm^{-1} .

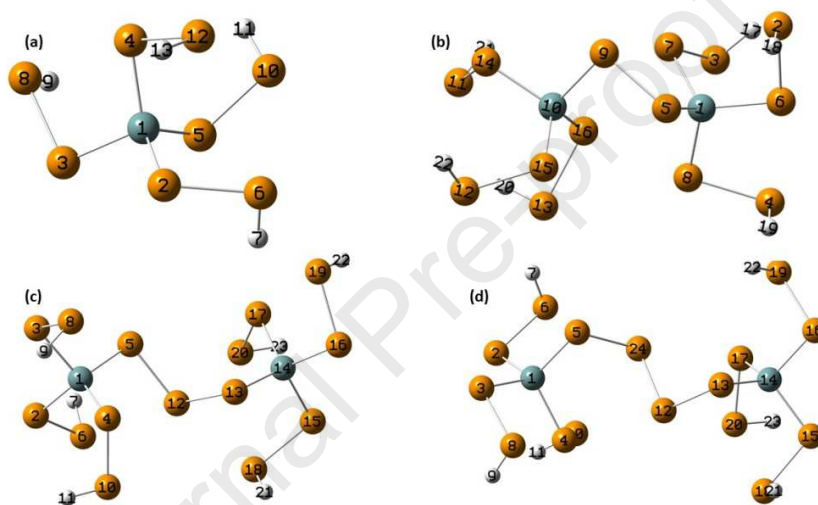


Figure 5. DF-optimized geometries of (a) $[\text{GeTe}_4]$, (b) $[\text{Ge-Te-Te-Ge}]$, (c) $[\text{Ge-Te-Te-Te-Ge}]$ et (d) $[\text{Ge-Te-Te-Te-Te-Ge}]$ clusters.

Table 2. Selected Raman and infrared-active vibrational modes for $[\text{GeTe}_4]$ cluster shown in Fig.5.

Calculated Frequency (cm^{-1})	Vibrational Mode	PED (%)	Cluster
131	$\nu_s \text{GeTe}_4$	$\nu(1,2)$: 18,2%, $\nu(1,3)$: 7,8%, $\nu(1,4)$: 20,3%, $\nu(1,5)$: 18,6%	Cluster a
145	$\nu(\text{Te})\text{-Te-Te-Te}$	$\nu(12, 24)$: 34,9%, $\nu(5,24)$: 11,2%, $\nu(12,13)$: 10,8%,	Cluster d

151	$\nu_{as}(\text{Ge})\text{-Te-Te-Te-(Ge)}$	$\nu(5,12): 24,1\%$, $\nu(12,13): 24,1\%$	Cluster c
154	$\nu_s(\text{Ge})\text{-Te-Te-Te-(Ge)}$	$\nu(5,12): 20,7\%$, $\nu(12,13): 20,8\%$	Cluster c
157	$\nu(\text{Ge})\text{-Te-Te-(Te)}$	$\nu(5,24) : 19,9\%$, $\nu(12,13): 27,7\%$	Cluster d
164	$\nu(\text{Ge})\text{-Te-Te-(Ge)}$	$\nu(5,9): 20,3\%$	Cluster b
216	$\nu_{as} \text{GeTe}_4$	$\nu(1,2) : 11,6\%$, $\nu(1,3) : 19,6\%$	Cluster a
232	$\nu_{as} \text{GeTe}_4$	$\nu(1,4): 11,1\%$, $\nu(1,5): 20,1\%$	Cluster a

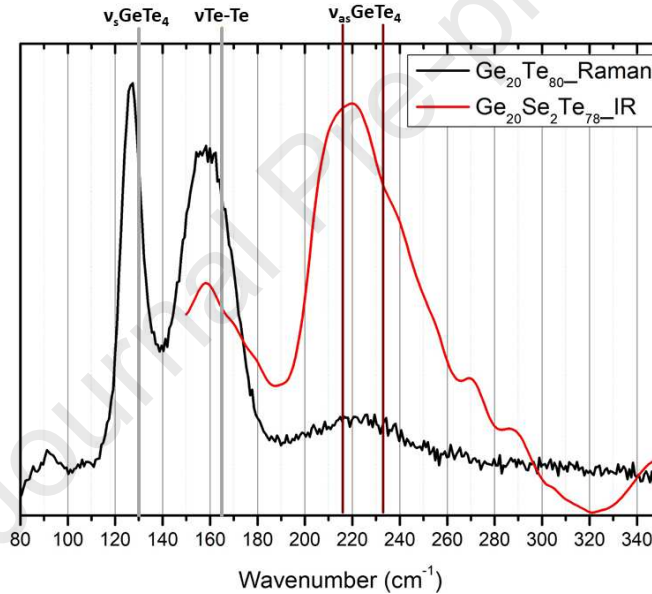


Figure 6. Raman spectrum of $\text{Ge}_{20}\text{Te}_{80}$ glass and Infrared spectrum of $\text{Ge}_{20}\text{Te}_{78}\text{Se}_2$ glass.

From DFT calculation, the selected modes of the Te-Te bond vibration range from 145 to 164 cm^{-1} (Table 2). The lowest frequency at 145 cm^{-1} corresponds to the Te-Te vibration surrounded by tellurium on both sides, whereas that at 164 cm^{-1} is attributed to the vibration of the Te-Te bond but this time surrounded by germanium on both side. The gradual shift to lower frequencies can be mainly explained by a predominant atom weight effect between Te and Ge. The 155 cm^{-1}

band observed in Raman spectra can be logically attributed to the stretching vibrational mode of Te-Te bonds.

From the results on binary glasses, the used of small clusters calculated by DFT calculation allow a good description of the structure. The same methodology is used for ternary glasses, with first, the focus on the rearrangement of the chain and second, on the reorganization of the tetrahedra, with the addition of Te or Se in the glassy matrix.

2.2.2. Ternary system $Ge_{20}Te_{80-x}Se_x$ (with x from 0 to 80)

- Mixed chains study

To provide a consistent study, different clusters were studied in this part with mixed chalcogen sequences linking two germanium of the type, Se-Te-Se, Te-Se-Te, Te-Te-Se, Se-Se-Te, for the ternary glasses. The selected clusters are represented in Figure 7 and are named respectively [Ge-Se-Te-Se-Ge], [Ge-Te-Se-Te-Ge], [Ge-Te-Te-Se-Ge] and [Ge-Se-Se-Te-Ge].

According to DFT calculations, the Raman and Infrared spectra of the clusters were calculated. To be clearer, only the vibrational modes of the mixed chains were extracted (Table 3).

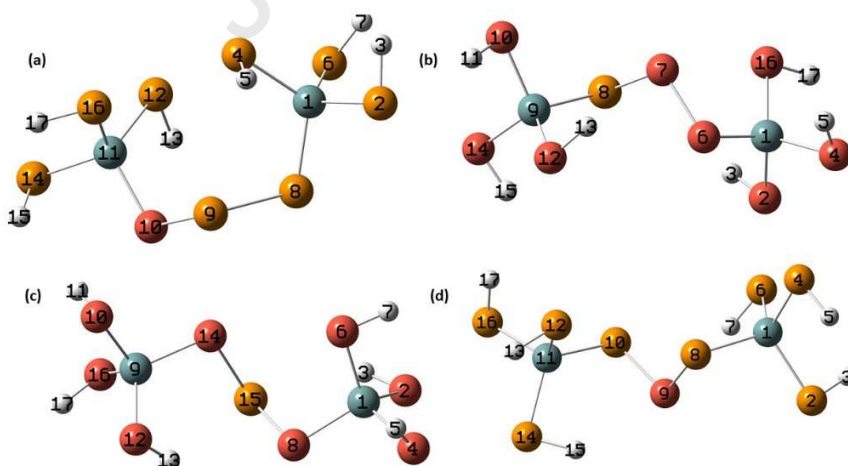


Figure 7. DF-optimized geometries of (a) [Ge-Se-Se-Te-Ge], (b) [Ge-Se-Se-Te-Ge], (c) [Ge-Se-Te-Se-Ge] and (d) [Ge-Te-Se-Te-Ge] clusters.

Table 3. Selected Raman and Infrared-active vibrational modes for mixed chain clusters shown in Fig. 8.

Calculated Frequency (cm^{-1})	Vibrational Mode	PED (%)	Cluster
157	$\nu\text{Te-Te}$	$\nu(6,7)$: 28,5%	Cluster a
208	$\nu_{\text{as}}(\text{Ge})\text{-Te-Se-Te-(Ge)}$	$\nu(7,8)$: 27,1%, $\nu(8,9)$: 15,2%	Cluster d
210	$\nu(\text{Se})\text{-Se-Te-(Ge)}$	$\nu(7,8)$: 34,0%	Cluster b
211	$\nu_{\text{s}}(\text{Ge})\text{-Te-Se-Te-(Ge)}$	$\nu(7,8)$: 12,6%, $\nu(8,9)$: 29,5%	Cluster d
212	$\nu_{\text{as}}(\text{Ge})\text{-Se-Te-Se-(Ge)}$	$\nu(8,15)$: 21,4%, $\nu(14,15)$: 22,4%	Cluster c
219	$\nu_{\text{s}}(\text{Te})\text{-Te-Se-(Ge)}$	$\nu(7,8)$: 32,0%	Cluster a
222	$\nu_{\text{s}}(\text{Ge})\text{-Se-Te-Se-(Ge)}$	$\nu(8,15)$: 20,7%, $\nu(14,15)$: 19,5%	Cluster c
266	$\nu(\text{Ge})\text{-Se-Se-(Te)}$	$\nu(7,8)$: 22,9%	Cluster b

The clusters [Ge-Te-Te-Se-Ge] and [Ge-Se-Se-Te-Ge] were studied to identify modes when Se or Te is inserted in a homopolar chain. For cluster (a), the presence of the modes $\nu\text{Te-Te}$ at 157 cm^{-1} and $\nu\text{Se-Te}$ at 219 cm^{-1} were indexed. When selenium is bonded to germanium (cluster b), the modes $\nu\text{Se-Te}$ at 210 cm^{-1} and the homopolar vibration $\nu\text{Se-Se}$ at 266 cm^{-1} were calculated. If the element added in the matrix binds to germanium, the homopolar mode is recorded.

The Se-Te-Se and Te-Se-Te modes are characteristic of the substitution of an atom by another, in the center of Se-Se or Te-Te homopolar chain. According to PED analysis, only the presence of the mixed mode Se-Te is observed between 208 and 222 cm^{-1} .

For the Se-rich part, the presence and rise of this band confirm the mode Se-Te. Moreover, by the decrease of the Se-Se band at 260 cm^{-1} , only the insertion of Te inside the Se-rich chain

(cluster c.) seems to be the arrangement present in the glassy matrix. Another statement can be made for tellurium-rich part, if selenium gets into the homopolar chain, the modes between 208 and 211 cm^{-1} would be shown on the Raman spectra. However, there is no mode at this frequency, the mixed $\nu\text{Se-Te}$ mode should not be present in the Te-rich part of the system in agreement with Ratkai *et al.*[15].

- Mixed tetrahedra study

In this part, we have defined mixed Se/Te clusters based on the GeSe_4 and GeTe_4 Td clusters depicted in Figure 3 and 5. As detailed in Figure 8, these mixed clusters are named: $\text{GeTe}_{8-x}\text{Se}_x$ with x varying from 0 to 8. For each x value, several arrangements of the chalcogenide atoms can be predicted. All possibilities are listed in Figure 8, the index number of the cluster together with its x value allow to find the details of the calculation results in a sum-up table provided in the supporting information section.

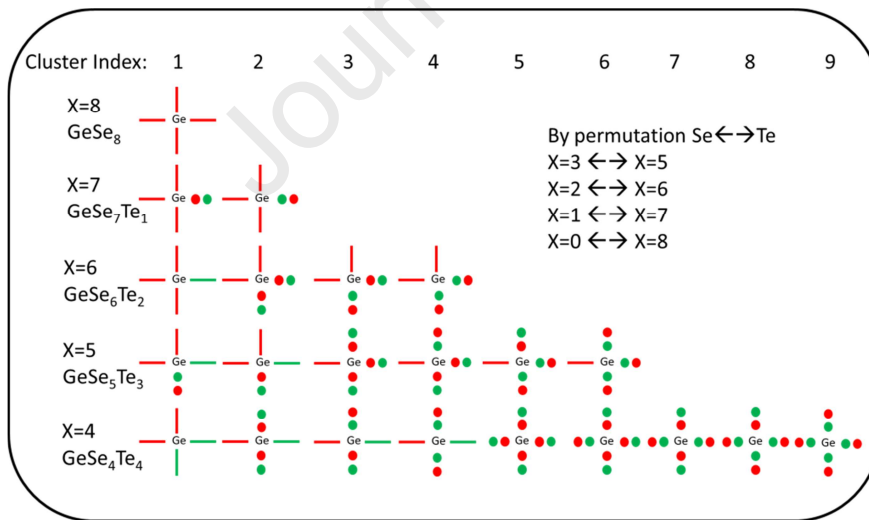


Figure 8. Schematic presentation of the DFT clusters calculated for the mixed Se,Te, Germanate tetrahedra vibrational mode study (Se are in red and Te in green)

As observed for the two binary compositions results, these simple clusters centered on the Ge atom give a reasonable description of the germanate units symmetric and asymmetric stretching modes. For the mixed (Te/Se)-Ge Td clusters of Figure 8, we have observed one symmetric stretching active in Raman (ν_s) and two asymmetric modes mainly observed in the IR spectra (ν_{as1} and ν_{as2}). In Figure 9, these stretching vibrations have been reported as a function of reduced masses of the calculated clusters. Reduced mass (1) corresponds to the entire reduced mass of the cluster taking into account the 8 chalcogenide atoms around the Ge atom. To calculate the reduced mass (2), only the chalcogenide atoms in the first shell around the Germanium are considered.

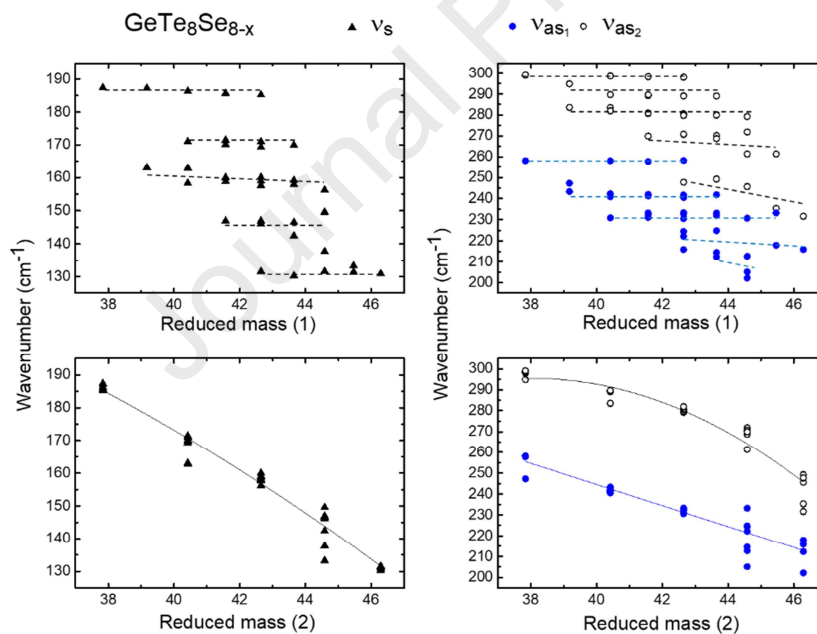


Figure 9. Calculated vibration wavenumbers of the internal modes of all the mixed Se/Te germanate tetrahedra presented in Figure 8. The data are traced as a function of the global reduced mass of the cluster (reduced mass (1) upper part of the figure) or as a function of a

reduced mass calculated only with the chalcogenide atoms in the first shell around the Germanium (reduced mass (2) lower part of the figure). The lines plotted are only visual guides.

The repartition of the vibrational frequencies as a function of the two reduced masses is largely different but coherent for the symmetric and asymmetric plotted modes. Looking at these frequencies as a function of the total reduced mass (1) of the cluster, there are some horizontal trends indicating that very similar vibration frequencies are calculated for clusters with very different respective amount of Se and Te. Conversely, by plotting the same data as a function of the reduced mass (2), which takes into account only the first shell of chalcogenide atoms around the germanium, a gradual decrease of the vibrational frequency is observed as the reduced mass increase.

In regard to these observations, one can conclude that the vibrational frequency of the tetrahedral internal modes is mostly sensitive to the chalcogen atoms directly bonded to the germanium. This observation was expected; however, it denotes that if the chalcogen introduction in the glassy matrix is not preferentially links to Ge, these modes are almost not sensitive to this change of composition.

3. DISCUSSION

A careful analysis of the data presented in this study allows to give some conclusions concerning the respective affinity of Ge, Se and Te along the pseudo-binary line $\text{GeSe}_4\text{-GeTe}_4$.

For selenium-rich glasses, the introduction of tellurium induces the appearance of a Raman mode at 210 cm^{-1} , attributed to Se-Te stretching, and a decrease of the large band at 260 cm^{-1} assigned to the Se-Se bonds. This is in accordance with the ^{77}Se NMR study reported by

Bouëssel du Bourg *et al.*[20] showing that the chemical shift at 860 ppm corresponding to the Se-Se-Se chains collapses upon tellurium addition in a GeSe₄ glassy matrix. Both studies denote that Se-Te-Se arrangements are formed preferentially to Se-Se-Te linkages. This is confirmed by NMR and vibrational characterizations focused on the germanate response. The ⁷³Ge NMR results has shown that adding 10% of tellurium in GeSe₄ does not modify the shape of the ⁷³Ge spectrum. Moreover, the Se/Te mixed Ge tetrahedral study by DFT calculations points out that if the chalcogen substitution is done on the second shell around the germanium, it does not affect significantly the internal mode of the tetrahedral units. It explains why the infrared spectra do not show significant spectral differences up to 20% of Se to Te substitution. Similarly, in Raman the symmetric stretching mode of GeS_{4/2} tetrahedral units peaking at 190 cm⁻¹ does not shift in frequency.

Finally, vibrational spectroscopy, ⁷⁷Se and ⁷³Ge NMR analysis are consistent and conclude that for the selenium-rich part of the pseudo-binary GeSe₄-GeTe₄, the Te is not connected directly to germanium and inserted in the vicinity of selenium chains.

Above 10% of Te in the glassy matrix, Se/Te mixed Ge tetrahedra can be expected has shown by the Raman mode at 170 cm⁻¹ corresponding well to a mixed-unit with only one Te atoms directly connected to Ge. Closer to the de-mixing zone, for the glass Ge₂₀Te₃₀Se₅₀ the IR response remains almost unchanged which could indicate that mixed germanate units with more than two Te in the vicinity of the germanium are not expected in agreement with Bouëssel du Bourg *et al.* In this case, the two strong Raman modes at 155 and 170 cm⁻¹, which dominates the Raman response for this particular composition, could be attributed to (Ge)-Se-Te-Te-(Ge) or (Ge)-Se-Te-Te-Se-(Ge) chains which modes are expected at these two wavenumbers.

For the tellurium-rich part, the Se-Te mode around 210 cm^{-1} is not observed in Raman. We have noted a gradual decrease of the $\nu_s\text{GeTe}_4$ around 130 cm^{-1} and an enlargement of the band pointing at 155 cm^{-1} which spread from 135 up to 175 cm^{-1} . In this spectral range, the DFT calculations have shown that we can expect Te-Te stretching but also the symmetric stretching of the Se/Te mixed Ge tetrahedra with 1, 2 or 3 selenium directly attached to germanium which were calculated around 145 , 160 and 170 cm^{-1} respectively. This presence of mixed tetrahedral units is also confirmed by the continuous change of the IR spectra which shift gradually towards higher wavenumbers upon insertion of Se in the Te-rich glasses. This trend of the IR response is also expected from the DFT calculations of the asymmetric stretching modes of mixed tetrahedral units. These findings agreed perfectly with the X-ray, neutron diffraction and extended X-ray fine structure (EXAFS) measurements reported by Ratkai *et al.*[15].

Finally, NMR and vibrational data reported in this study can confirm and clarify a whole structural description of the $\text{GeSe}_4 / \text{GeTe}_4$ glassy system. As observed from both sides of the demixing zone, all studies point out that the highest affinity of Se with Ge governs the glassy structure. It denotes that a homogeneous glassy network, i.e. with an amount of Se/Te mixed germanate tetrahedral units following the glass composition, might be obtained only for the Te-rich part of the glassy system. For the selenium-rich part, mixed Se-(Te)_x-Se chains will be preferred.

4. CONCLUSION

Vibrational spectra and NMR study allow to make a structural assessment of the $\text{Ge}_{20}\text{Te}_{80-x}\text{Se}_x$ glass series. For selenium-rich glasses, when tellurium is added, it would tend to be inserted into the Se-Se chains, to form mixed chains, of the Se-Te type. However, above a certain percentage

of tellurium, it would eventually bind to germanium to form mixed tetrahedra, like those of [GeTeSe] clusters. In the case of tellurium-rich glasses, it would appear that when selenium is added, given the strong affinity of selenium with germanium, there would be the formation of Se/Te mixed Ge tetrahedra connected to each other by Te-Te homopolar chains. Moreover, no vibrational signature of the mixed-chain modes (210 cm^{-1}) is observed, confirming the only presence of the vibration mode $\nu\text{Te-Te}$.

ASSOCIATED CONTENT

Supporting Information.

-A table containing all calculated values for each mixed $\text{GeTe}_{8-x}\text{Se}_x$ clusters depicted in Figure 8 and plotted in Figure 9 (PDF)

AUTHOR INFORMATION

Corresponding Author

*E-mail: marc.dussauze@u-bordeaux.fr, virginie.nazabal@univ-rennes1.fr

Author Contributions

The manuscript was written through contributions of all authors. All authors have given approval to the final version of the manuscript.

Data Availability Statement

The data that support the findings of this study are available from the corresponding author upon reasonable request.

ACKNOWLEDGMENT

The authors gratefully acknowledge the financial support of: l'Agence Nationale de la Recherche for the project IRTeGlass (ANR-14-CE07-0013-03), IDEX Bordeaux (Cluster of Excellence LAPHIA and the allocated grant referred to as ANR-10-IDEX-03-03), and the CNRS project EMERGENCE @INC2019. All IR and Raman experiments have been performed at the platform SIV at University of Bordeaux, funded by the FEDER and the Region Aquitaine.

ABBREVIATIONS

NMR, Nuclear magnetic resonance; DFT, Density Functional Theory; EXAFS, Extended X-Ray Absorption Fine Structure; IR, Infrared; XRD, X-ray Diffraction; DSC, Differential scanning calorimetry; QCPMG, Quadrupolar Carr-Pucell-Meiboom-Gill echo sequence; VOCS, Variable Offset Cumulative Spectrum; PED, Potential Energy Distribution.

REFERENCES

- [1] S.B. Bhanu Prashanth, S. Asokan, Composition dependent electrical switching in glasses—the influence of network rigidity and thermal properties, *Solid State Commun.* 147 (2008) 452–456. <https://doi.org/10.1016/j.ssc.2008.07.005>.
- [2] R. Ganesan, A. Srinivasan, K.N. Madhusoodanan, K.S. Sangunni, E.S.R. Gopal, Composition Dependence of the Glass Transition in Ge–Se–Te Glasses, *Phys. Status Solidi B.* 190 (1995) K23–K26. <https://doi.org/10.1002/pssb.2221900231>.
- [3] K.A. Rubin, M. Chen, Progress and issues of phase-change erasable optical recording media, *Thin Solid Films.* 181 (1989) 129–139. [https://doi.org/10.1016/0040-6090\(89\)90479-3](https://doi.org/10.1016/0040-6090(89)90479-3).
- [4] P. Sharma, S.C. Katyal, Far-infrared transmission and bonding arrangement in Ge₁₀Se_{90-x}Te_x semiconducting glassy alloys, *J. Non-Cryst. Solids.* 354 (2008) 3836–3839. <https://doi.org/10.1016/j.jnoncrysol.2008.05.010>.

- [5] E.M. Vinod, A.K. Singh, R. Ganesan, K.S. Sangunni, Effect of selenium addition on the GeTe phase change memory alloys, *J. Alloys Compd.* 537 (2012) 127–132. <https://doi.org/10.1016/j.jallcom.2012.05.064>.
- [6] S. Maurugeon, B. Bureau, C. Boussard-Plédel, A.J. Faber, X.H. Zhang, W. Geliesen, J. Lucas, Te-rich Ge–Te–Se glass for the CO₂ infrared detection at 15 μ m, *J. Non-Cryst. Solids.* 355 (2009) 2074–2078. <https://doi.org/10.1016/j.jnoncrysol.2009.01.059>.
- [7] S. Danto, P. Houizot, C. Boussard-Plédel, X.-H. Zhang, F. Smektala, J. Lucas, A Family of Far-Infrared-Transmitting Glasses in the Ga–Ge–Te System for Space Applications, *Adv. Funct. Mater.* 16 (2006) 1847–1852. <https://doi.org/10.1002/adfm.200500645>.
- [8] E.L. Gjersing, S. Sen, B.G. Aitken, Structure, Connectivity, and Configurational Entropy of GexSe100–x Glasses: Results from ⁷⁷Se MAS NMR Spectroscopy, *J. Phys. Chem. C.* 114 (2010) 8601–8608. <https://doi.org/10.1021/jp1014143>.
- [9] T.G. Edwards, S. Sen, E.L. Gjersing, A combined ⁷⁷Se NMR and Raman spectroscopic study of the structure of GexSe1–x glasses: Towards a self consistent structural model, *J. Non-Cryst. Solids.* 358 (2012) 609–614. <https://doi.org/10.1016/j.jnoncrysol.2011.11.008>.
- [10] B. Bureau, J. Troles, M. Le Floch, P. Guénot, F. Smektala, J. Lucas, Germanium selenide glass structures studied by ⁷⁷Se solid state NMR and mass spectroscopy, *J. Non-Cryst. Solids.* 319 (2003) 145–153. [https://doi.org/10.1016/S0022-3093\(02\)01911-7](https://doi.org/10.1016/S0022-3093(02)01911-7).
- [11] M. Kibalchenko, J.R. Yates, C. Massobrio, A. Pasquarello, Structural Composition of First-Neighbor Shells in GeSe₂ and GeSe₄ Glasses from a First-Principles Analysis of NMR Chemical Shifts, *J. Phys. Chem. C.* 115 (2011) 7755–7759. <https://doi.org/10.1021/jp201345e>.
- [12] M. Micoulaut, A. Kachmar, M. Bauchy, S. Le Roux, C. Massobrio, M. Boero, Structure, topology, rings, and vibrational and electronic properties of GexSe1–x glasses across the rigidity transition: A numerical study, *Phys. Rev. B.* 88 (2013) 054203. <https://doi.org/10.1103/PhysRevB.88.054203>.
- [13] K. Sykina, E. Furet, B. Bureau, S. Le Roux, C. Massobrio, Network connectivity and extended Se chains in the atomic structure of glassy GeSe₄, *Chem. Phys. Lett.* 547 (2012) 30–34. <https://doi.org/10.1016/j.cplett.2012.07.077>.
- [14] P. Jóvári, I. Kaban, B. Bureau, A. Wilhelm, P. Lucas, B. Beuneu, D.A. Zajac, Structure of Te-rich Te–Ge–X (X = I, Se, Ga) glasses, *J. Phys. Condens. Matter.* 22 (2010) 404207. <https://doi.org/10.1088/0953-8984/22/40/404207>.
- [15] L. Rátkai, C. Conseil, V. Nazabal, B. Bureau, I. Kaban, J. Bednarcik, B. Beuneu, P. Jóvári, Microscopic origin of demixing in Ge₂₀SexTe_{80–x} alloys, *J. Alloys Compd.* 509 (2011) 5190–5194. <https://doi.org/10.1016/j.jallcom.2011.02.032>.
- [16] R. Svoboda, D. Brandová, J. Málek, Thermal behavior of Ge₂₀Se_yTe_{80–y} infrared glasses (for y up to 8 at.%), *J. Alloys Compd.* 680 (2016) 427–435. <https://doi.org/10.1016/j.jallcom.2016.04.165>.
- [17] R. Svoboda, D. Brandová, M. Chromčíková, M. Setnička, J. Chovanec, A. Černá, M. Liška, J. Málek, Se-doped GeTe₄ glasses for far-infrared optical fibers, *J. Alloys Compd.* 695 (2017) 2434–2443. <https://doi.org/10.1016/j.jallcom.2016.11.139>.
- [18] J. Sun, Q. Nie, X. Wang, S. Dai, X. Zhang, B. Bureau, C. Boussard, C. Conseil, H. Ma, Structural investigation of Te-based chalcogenide glasses using Raman spectroscopy, *Infrared Phys. Technol.* 55 (2012) 316–319. <https://doi.org/10.1016/j.infrared.2012.03.003>.

- [19] A.H. Moharram, M.A. Hefni, A.M. Abdel-Baset, Short and intermediate range order of $\text{Ge}_{20}\text{Se}_{80-x}\text{Te}_x$ glasses, *J. Appl. Phys.* 108 (2010) 073505. <https://doi.org/10.1063/1.3488907>.
- [20] L.B. du Bourg, C. Roiland, L. le Pollès, M. Deschamps, C. Boussard-Plédel, B. Bureau, C.J. Pickard, E. Furet, Impact of Te on the structure and ^{77}Se NMR spectra of Se-rich Ge–Te–Se glasses: a combined experimental and computational investigation, *Phys. Chem. Chem. Phys.* 17 (2015) 29020–29026. <https://doi.org/10.1039/C5CP04416B>.
- [21] E. Petracovschi, B. Bureau, A. Moreac, C. Roiland, J.-L. Adam, X.-H. Zhang, L. Calvez, Structural study by Raman spectroscopy and ^{77}Se NMR of GeSe_4 and $80\text{GeSe}_2\text{--}20\text{Ga}_2\text{Se}_3$ glasses synthesized by mechanical milling, *J. Non-Cryst. Solids.* 431 (2016) 16–20. <https://doi.org/10.1016/j.jnoncrysol.2015.04.015>.
- [22] A.P.M. Kentgens, R. Verhagen, Advantages of double frequency sweeps in static, MAS and MQMAS NMR of spin $I=3/2$ nuclei, *Chem. Phys. Lett.* 300 (1999) 435–443. [https://doi.org/10.1016/S0009-2614\(98\)01402-X](https://doi.org/10.1016/S0009-2614(98)01402-X).
- [23] D. Massiot, I. Farnan, N. Gautier, D. Trumeau, A. Trokiner, J.P. Coutures, ^{71}Ga and ^{69}Ga nuclear magnetic resonance study of $\beta\text{-Ga}_2\text{O}_3$: resolution of four- and six-fold coordinated Ga sites in static conditions, *Solid State Nucl. Magn. Reson.* 4 (1995) 241–248. [https://doi.org/10.1016/0926-2040\(95\)00002-8](https://doi.org/10.1016/0926-2040(95)00002-8).
- [24] E.I. Kamitsos, A.P. Patsis, M.A. Karakassides, G.D. Chryssikos, Infrared reflectance spectra of lithium borate glasses, *J. Non-Cryst. Solids.* 126 (1990) 52–67. [https://doi.org/10.1016/0022-3093\(90\)91023-K](https://doi.org/10.1016/0022-3093(90)91023-K).
- [25] S. Sen, Z. Gan, Chemical order around Ge atoms in binary germanium selenide glasses: Results from ^{73}Ge solid-state NMR spectroscopy at 19.6 Tesla, *J. Non-Cryst. Solids.* 356 (2010) 1519–1521. <https://doi.org/10.1016/j.jnoncrysol.2010.04.043>.
- [26] K.S. Andrikopoulos, S.N. Yannopoulos, A.V. Kolobov, P. Fons, J. Tominaga, Raman scattering study of GeTe and $\text{Ge}_2\text{Sb}_2\text{Te}_5$ phase-change materials, *J. Phys. Chem. Solids.* 68 (2007) 1074–1078. <https://doi.org/10.1016/j.jpcs.2007.02.027>.
- [27] S. Sen, E.L. Gjersing, B.G. Aitken, Physical properties of $\text{Ge}_x\text{As}_{2x}\text{Te}_{100-3x}$ glasses and Raman spectroscopic analysis of their short-range structure, *J. Non-Cryst. Solids.* 356 (2010) 2083–2088. <https://doi.org/10.1016/j.jnoncrysol.2010.08.013>.

Study of the $\text{Ge}_{20}\text{Te}_{80-x}\text{Se}_x$ glassy structures by combining solid state NMR, vibrational spectroscopies and DFT modelling

Claudia Gonçalves^{1,2}, Raphaël Mereau², Virginie Nazabal^{1,}, Catherine Boussard-Pledel¹,
Claire Roiland¹, Eric Furet³, Michaël Deschamps⁴, Bruno Bureau¹, Marc Dussauze^{2,*}*

¹ Institut des Sciences Chimiques de Rennes, UMR 6226 CNRS, Equipe Verres & Céramiques,
Université Rennes 1, Campus de Beaulieu, 35042 Rennes, France

² Institut des Sciences Moléculaires, Université de Bordeaux, CNRS UMR 5255, F-33400
Talence, France

³ Institut des Sciences Chimiques de Rennes, UMR 6226 CNRS, Ecole Nationale Supérieure de
Chimie de Rennes, 35708 Rennes, France

⁴ CNRS, CEMHTI UPR3079, Orléans University, Orléans 45100, France

Highlights:

- A multi technical approach (Raman, IR, NMR and DFT calculation) to describe mixed selenide-telluride glassy structures.
- Structural description for both the selenide and telluride rich part the system.
- Local structural entities and their interconnections description in this GeSeTe glassy structures.

Study of the $\text{Ge}_{20}\text{Te}_{80-x}\text{Se}_x$ glassy structures by combining solid state NMR, vibrational spectroscopies and DFT modelling

Claudia Gonçalves^{1,2}, Raphaël Mereau², Virginie Nazabal^{1,}, Catherine Boussard-Pledel¹,
Claire Roiland¹, Eric Furet³, Michaël Deschamps⁴, Bruno Bureau¹, Marc Dussauze^{2,*}*

¹ Institut des Sciences Chimiques de Rennes, UMR 6226 CNRS, Equipe Verres & Céramiques,
Université Rennes 1, Campus de Beaulieu, 35042 Rennes, France

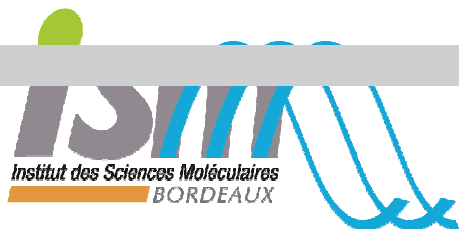
² Institut des Sciences Moléculaires, Université de Bordeaux, CNRS UMR 5255, F-33400
Talence, France

³ Institut des Sciences Chimiques de Rennes, UMR 6226 CNRS, Ecole Nationale Supérieure de
Chimie de Rennes, 35708 Rennes, France

⁴ CNRS, CEMHTI UPR3079, Orléans University, Orléans 45100, France

Graphical abstract legend:

A multi technical approach (Raman, IR, NMR and DFT calculation) to describe mixed selenide-telluride glassy structures.



3rd December 2020
University of Bordeaux FRANCE

Declaration of interests

To,
The Editor-in-chief,
Journal of Solid State Chemistry

The authors declare that they have no known competing financial interests or personal relationships that could have appeared to influence the work reported in this paper.

A handwritten signature in black ink, appearing to be 'Dr. Dussauze Marc'. The signature is stylized and somewhat abstract, with a long horizontal stroke extending to the right.

Dr. Dussauze Marc

Journal Pre-proof